Determine The Feasibility For Dissimilar Materials: Al Alloy Al-5400 And Steel 304l By Friction Stir Welding

Shantanu Madhukar Kadam[1]*, Dr. Sunil K. Somani[2], Dr. H. S. Patil[3]

Abstract:

A sort of solid welding called friction stir welding attache's two items without melting them. It makes use of a temporary tool. Heat is produced by the friction between the workpiece and the tool. The metal is not melted by this heat; it merely softens it. Since there are significant differences in the physical and chemical qualities of the components that need to be bonded, fusion welding is not an option in many industries, such as those in the automobile, aircraft, shipbuilding, and electronics. For joining purposes, the tool moves over the softer surface. The range of welding is expanding daily in accordance with client demands. The impact of penetration depth at 50 RPM is now being researched, and it has been discovered that the deeper the penetration, the more stress the work piece causes. Additionally, due to increased friction, the heat at the contact surface has increased, yet the temperature required to melt the work piece is sufficient to form the weld.

Keywords: Friction Stir Welding, Workpiece, AL Alloy, PCBN tool, FSW process analysis, Mechanical properties, Microstructural properties

DOI Number: 10.4704/nq.2022.20.14. NQ880147 **Neuroquantology 2022; 20(14):1046-1055**

1. INTRODUCTION

Friction stir welding (FSW) was developed in the early 1990s by Thomas and colleagues at the UK's The Welding Institute (TWI). The advantages of FSW over conventional fusion welding methods are considerable. Regulated low heat input, diminished heat affected zone (HAZ) degradation, diminished corrosion sensitization, diminished thermal distortion, and diminished residual stress are the key contributors to this [2, 3]. FSW offers significant benefits over fusion welding in many industrial applications because of its capacity for remote welding and eco-friendliness [2]. To mix the components within, a rotating tool made of a tougher, non-consumable material is inserted into the workpiece and moved over the abutting surfaces. A plasticized zone forms around the tool pin as a result of frictional heat generated by tool rotation, allowing material to flow and create the joint. The novel connecting technique Prevents the needed workpieces from melting, producing a weld with wrought microstructure.

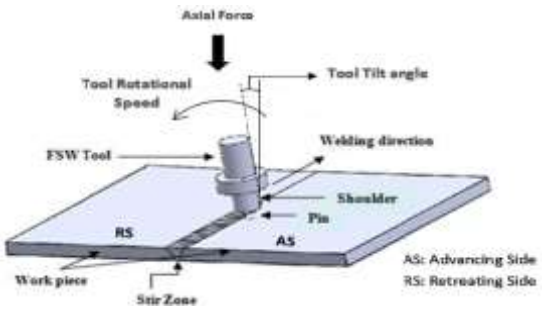

Figure 1: Schematic diagram of FSW [4]

FSW is being investigated as a practical method to fix flaws in metallic constructions on the basis of the aforementioned concept [4–7]. Thomas et al. proposed that abutting sides of a fracture may potentially be brought together to perform component mending [4] as an extension of the friction stirring technique. It

***Corresponding Author**:- Shantanu Madhukar Kadam
Address:- *[1]Research scholar, Oriental University, Indore
[2]Vice- Chancellor, Oriental University, Indore
[3]Professor and Faculty, Mechanical Engg, Depart. GIDC Degree Engineering College, Abrama, Navasari University.
Relevant conflicts of interest/financial disclosures: The authors declare that the research was conducted in the absence of any commercial or financial relationships that could be construed as a potential conflict of interest

was advised to use FSW to fix a variety of fracture types in aluminium alloys, including full thickness and partial penetration fractures in the parent material, heat affected zone, or weld zone. Arbegast and Hartley have also suggested FSW as a repair method for aerospace materials that are crack-sensitive [5]. Following this, super alloys, ferrous and non-ferrous alloys, as well as fracture repair and crack mitigation in metal matrix composites, were added to the list of materials acceptable for damage restoration via the FSW approach [6]. Through a lab-scale experiment on filling up simulated cracks in stainless steel (SS) plates, the potential utility of FSW for damage restoration was further expanded to nuclear applications. The purpose of the simulated cracks on the SS plates was to mimic the damage that corrosion and radiation cause to stainless structures used in the nuclear industry [7, 8]. Many sectors, including shipbuilding, oil & gas, nuclear power, and aviation, are seen to have application potential for FSW-based damage restoration procedures. Therefore, the pre-existing crack in the metallic structure can be fixed by applying FSW along it. FSW has mostly been used for joining and repairing materials, such as alloys of copper, magnesium, and aluminium [9].

This is because the capacity of the tool material to tolerate heat, stress, and abrasion is not as constrained by the lower strengths and melting temperatures of these metallic systems. Due to its great strength and melting point, steel requires high temperatures to perform FSW. This calls for the usage of complex tool materials capable of withstanding increased strain, temperature, and abrasion resistance during the stirring process. FSW of steel has started to receive a lot of attention and become more practical for connecting alloys of steel and aluminium with the development of new tool technology [8, 10-13, 14 -22]. Although other cutting-edge methods of damage restoration, such cold spraying and laser aided spot welding, should also be employed, a preliminary analysis of FSW's efficacy in fixing cracks in austenitic stainless steel has been carried out here. In preparation for the potential industrial deployment of the FSW-based damage repair technique, this is expected to contribute essential data to the database. One of the most often used materials for structural reasons is 304L austenitic stainless steel, which is used in a variety of industries, including the chemical, nuclear, food processing, and petrochemical ones. Despite being resistant to corrosion and high temperature deterioration, 304L stainless steel structures frequently fracture as a result of the corrosive service environment and other associated elements, creating significant challenges for the structure's integrity and maintenance. The current study uses a method based on process-microstructure mechanical property correlations to investigate the efficacy of FSW as a method to repair fractures in 304L stainless steel plates. The subject of fracture reparability in austenitic SS by FSW technique has not received much study attention. Ross et al. [7] examined the use of friction stir processing [8] to fix surface fractures caused by a simulated environment for corrosion in 25 mm thick 304L stainless steel plates.

In the current investigation FSW was carried out using PCBN and a special temperature-controlled algorithm to maintain the tool temperature at 25°C while FSW was being carried out on simulated fractures with straight geometry (in the form of wire cut straight holes) in 10-mm thick 304L SS plates. A 50 rpm traverse speed was adopted. This fundamental study seeks to show the potential of FSW in the repair of damaged stainless steel plate using meticulous microstructural characterization and mechanical testing.

2. LITERATURE SURVEY

For FSW, high-speed steel is a typical tool material (HSS). Soft metals like aluminium, copper, and their alloys are routinely joined together using this kind of tool [23–25]. Tool wear can be decreased by adjusting process parameters [26]. Due to their inability to produce the required temperature, endure temperatures beyond 950 °C, or tolerate abrasive wear, HSS tools are useless for welding steels [27–29]. Steel joining tools need to be highly durable, hard and strong, and able to bear all kinds of wear. Because of all these qualities, commercially pure tungsten (Cp-W) and polycrystalline cubic boron nitride are the materials used for tools today (PCBN).

2.1 Tools using refractory metals for FSW

Metals having high melting points and resistance to wear are referred to as refractory me-

tals. Because of its high melting point, the refractory metal tool cannot be made using traditionnal metal-based forming processes [30]. Metal injection moulding is used to make refracttory metal tools. The cost of metal will be significantly greater than if HSS tools were used because of this labor-intensive operation. Today, silicon nitride, tungsten carbide, tungsten lanthanide, and tungsten carbide cobalt alloy are most important refractory metal FSW tools employed [31, 32]. The properties of the refractory metals are shown in Figure 2.

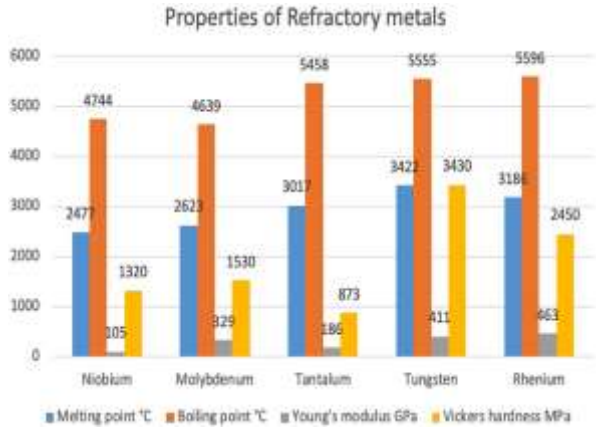

Figure 2: Properties of refractory metals

Tungsten and molybdenum tools were used in the early phases of FSW welding steel. The primary drawback of these FSW tools is that when they pierce steel, they fracture and distort [33]. The high tool material ductile-to-brittle transition temperatures and the tremendous axial force used to press the tool into the steel are to blame for the deformations. Due to all of these problems, tungsten-rhenium (W-25%Re), a new refractory tool material, was introduced to replace these metals. The rhenium alloying component gives the tungsten-rhenium alloy higher wear resistance and lower ductile-to-brittle transition temperatures than molybdenum and tungsten [34, 35]. Additionally, the tool's damage from the welding of steels has not yet been fully fixed.

2.2 Synthetic Material as an FSW Tool

One of the finest Carbon Boron Nitride products for friction stir welding, machining, and cutting operations is polycrystalline cubic boron nitride (PCBN). Techniques like as sintering or frottage can be utilised to create PCBN [36–38]. This sintering process needs binder stages, high temperatures, and pressures. The binder phase involves the utilisation of ceramics like aluminium oxide, titanium carbide, and titanium nitride as well as metals like nickel and copper [39–43]. PCBN has tremendous hardness, yet the only hard material that is harder than PCBN is diamond. Compared to diamond, PCBN can withstand much greater temperatures. Excellent toughness, thermal shock resistance, and chemical wear resistance are further benefits of PCBN [44–46]. These qualities led to PCBN tools being widely used in machining applications, such as friction stir welding. Numerous studies on PCBN tools are carried out. The pin and shoulder profiles are emphasised a lot, along with how they affect the weld's mechanical properties. [47].

According to studies, PCBN may be used to implement austenitic, ferritic, martensitic, and duplex stainless steels as well as other alloy and stainless steels. PCBN gives a significantly better joint with constant microstructures than FSW tools composed of refractory metals [48, 49]. In several experiments, less hard steel alloys with up to a 12 mm thickness were joined using PCBN-tungsten alloy welding equipment. Despite using the same metals, these tools kept deforming [50]. The majority of consideration today is given to tools built of superalloys. FSW commonly uses cobalt- or nickel-based superalloys [51–53]. Furthermore, these are not long-term fixes for sturdier connections, lower tool failure rates, or cheaper steel welding procedures. Recent research suggests that a hybrid welding strategy is the better option. These techniques may be used to weld hard alloys using standard tools, such as the tungsten carbide tool for AISI 5400 stainless steel plates [54, 55].

3. MATERIALS AND TOOLS

3.1 Materials

Scheduled for processing and friction stir welding are tool materials. The list of intended tool materials should not be regarded as comprehendsive because many publications state that the tool material is confidential or fail to identify it. For convenient reference, Table 1 lists the present tool materials for friction stirring the pertinent materials and thicknesses. These numbers have been compiled from the listed literature sources.

Table 1: A list of the materials used in friction stir welding tools today, along with their forging temperatures.

Alloys	Tool materials	Forging temperature in ^0c
Aluminum alloys	Tool steel, WC-Co	440-560
Titanium alloys	Tungsten alloys	700-360
Stainless steels	PCBN, tungsten alloys	860-1030
Low-alloy steel	WC, PCBN	650-810

3.1.1 Tool Steels

The most typical tool material used in FSW is tool steel. This is because tool steels can easily friction stir aluminium alloys, which are the subject of the majority of published FSW studies. Tool steel has the benefits of being readily available and machinable, affordable, and having well-established material qualities.

3.2 Material Properties:

Because the temperature affects the stresses and strains in the weld, the FSW process rely on correct temperature estimations. Thermal conductivity, specific heat, and density of 304L steel plates are all influenced by temperature. Due to the limits of the data obtained in the literature, Young's modulus and the coefficient of thermal expansion of the plates are assumed to be constant.

3.1.1 Workpiece Material Properties

Table 2: Material properties of the plates

Material Properties of the Plates	Steel	AL Alloy
Young's modulus	193 GPa	71GPa
Poisson's ratio	0.3	0.33
Coefficient of thermal expansion	18.7 μm/m °C	23 μm/m °C

3.1.2 Bilinear Isotropic Hardening Constants (TB, BISO)

Table 3: Bilinear Isotropic Hardening Constants (TB, BISO)

Bilinear Isotropic Hardening Constants (TB,BISO)	Steel	AL Alloy
Yield stress [J]	290 MPa	280 MPa
Tangent modulus [J]	2.8 GPa	5Gpa

3.1.3 Temperature Dependent Material Properties

Table 4: Steel's Material Properties as a Function of Temperature

Properties	Values					
Temperature (°C)	0	200	400	600	800	1000
Thermal Conductivity (W/m °C)	16	19	21	24	29	30
Specific Heat (J/Kg °C)	500	540	560	590	600	610
Density (Kg/m^3)	7894	7744	7631	7518	7406	7406

Table 5: AL Alloy's Temperature Dependent Material Characteristics

Properties	Values					
Temperature (°C)	0	200	400	600	800	1000
Thermal Conductivity (W/m °C)	144	175	185	205	225	250
Specific Heat (J/Kg °C)	700	740	760	790	800	810
Density (Kg/m^3)	2700	2690	2670	2650	2650	2650

3.14 Material Properties of the PCBN Tool

Table 6: Material Characteristics of the PCBN Tool

Young modulus	680 GPa
Poisson's ratio	0.22
Thermal Conductivity	100 W/m °C
Specific Heat	750 J/Kg °C
Density	4280 Kg/m^3

4. PERFORMANCE ANALYSIS

4.1 Friction Stir Welding (FSW) Simulation:

The modelling of the friction stir welding (FSW) process was described in this study. The surface interaction between the tool and the workpiece, heat production from friction, and plastic deformation are a few of the FSW properties that are investigated. A nonlinear direct coupled field analysis is conducted since the mechanical and thermal behaviours of the FSW process are coupled and dependent upon one another. The following qualities and abilities are highlighted:

- Utilizing coupled-field solid elements for direct structural-thermal analysis,
- plastic heat production in coupled-field elements,
- Utilizing coupled-field solid elements for direct structural-thermal analysis,
- Surface-projection-based contact technique
- Bonding-capable contact components

In the FSW process, the tool is frequently made of a material that is more durable than the material of the workpiece being welded. Aluminum and other soft workpiece materials were for-

merly utilised with FSW. FSW is now achievable with high-temperature materials like stainless steel thanks to the development of tools constructed of extremely abrasive materials such polycrystalline cubic boron nitride (PCBN). In this case, a cylindrical PCBN tool is modelled.
To mimic the clamping ends, the workpiece sides parallel to the weld line are restrained in all directions. To imitate support at the bottom, the workpiece's bottom side is restrained in the perpendicular (z) direction. Every surface of the model has heat losses incorporated. The weld centerline serves as the focal point of all symmetric boundary conditions.

Three load stages are used in the simulation, each of which corresponds to one of the three processes in the FSW process (plunge, dwell, and traverse).

4.2 Workpiece and Tool Modeling:

The workpiece consists of two rectangular plates identical to those in the reference model. By lowering the dimensions, the simulation time has been drastically reduced. The plate is 80x 40x 4mm. The diameter of the tool's shoulder is 10 mm.

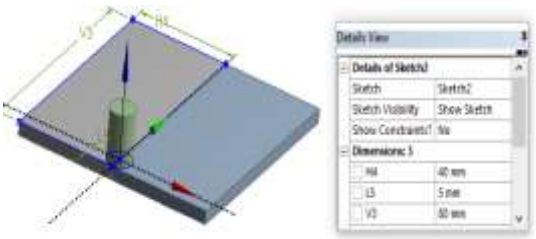

Figure 3: 3-D Workpiece and Tool Model

4.3 Meshing

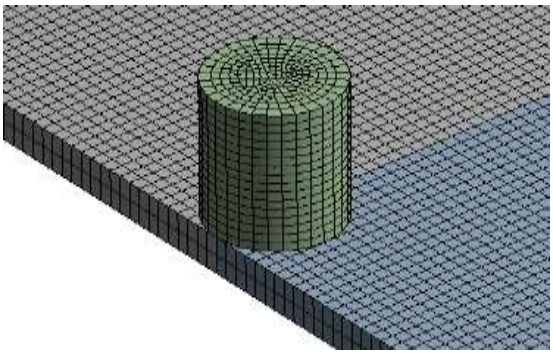

Figure 4: Workpiece and tool 3-D meshed models

4.4 SOLID226: 3-D 20-Node Coupled-Field Solid

Twenty nodes, each with a maximum of six degrees of freedom, make up the element. Elasticity, plasticity, hyperelasticity, viscoelasticity, viscoplasticity, creep, massive strain, high deflection, and the effects of stress stiffening are all structural properties. Furthermore, it allows for the employment of mixed formulations to imitate the deformations of both nearly incompressible elastoplastic and completely incompressible hyperelastic materials.
One of the properties of piezoresistive materials is the piezoresistive effect. Two examples of piezoelectric properties are direct and reverse piezoelectric effects. An attribute of electrostatic structures is electrostatic force coupling. There are several thermoelectric effects, including Seebeck, Peltier, Thomson, and Joule heating. In dynamic studies, the piezocaloric effect includes structural-thermal capacity in addition to thermal expansion. There is a chance that research utilising structural degrees of freedom will uncover the Coriolis Effect. It is feasible to analyse the thermoplastic effect using structural and thermal degrees of freedom.

One of the properties of structural magnetism is magnetic force coupling. Magnetic force coupling, eddy currents, and velocity effects are examples of structural-electromagnetic capabilities in a transient investigation.

A characteristic known as joule heating exists in thermal-magnetic and thermal-electromagnetic materials. Eddy current effects and velocity effects in static and transient analyses are two further instances of thermal-electromagnetic capabilities.

Table 7: SOLID226 Coupled-Field Analyses

Coupled-Field Analysis	KEYOPT	DOF Label	Force Label	Reaction Solution	Analysis Type
Structural Thermal	11	UX, UY, UZ, TEMP	FX, FY, FZ, HEAT	Force, Heat Flow	Static Full Harmonic Full Transient

The effects of hydrostatic stress-migration and diffusion expansion may be examined using structural and diffusion degrees of freedom. For study with thermal and diffusion degrees of freedom, the thermo-migration effect (Soret effect) and the saturation concentration effects at different temperatures are presented. The

degrees of freedom for electrical and diffusion are compatible with assessments of the electro-migration effect.

4.5 Loading & Boundary Conditions:

4.5.1 Thermal Boundary Conditions:

The frictional and plastic heat generated during the FSW process quickly dissipates in remote portions of the plates. Heat loss from the top and side surfaces of the workpiece to the environment is caused by convection and radiation. Additionally, there are conductivity losses from the base of the workpiece to the backing plate.

Figure 5: Thermal Boundary Conditions

Convection coefficient for the workpiece and tool is 30 W/m2°C. The output temperature is affected by this coefficient. A smaller coefficient raises the model's output temperature. It is anticipated that the conductive heat loss through the workpiece's bottom surface would have a high overall heat-transfer coefficient of 300 W/m2 °C (about ten times the convective coefficient). The bottom surface of the workpiece is also regarded as a convection surface to simulate conduction losses. Radiation heat losses are disregarded since there is little radiation-related heat loss. The model is given a 25 °C starting temperature. There are no places in the model where temperature boundary requirements are applied.

4.5.2 Mechanical Boundary Conditions

Each plate is clamped to secure the workpiece. The plates' clamped sections are restrained in all directions. To mimic support at the base of the plates, all of the workpiece's bottom nodes are restricted to pointing in a perpendicular direction (z direction).

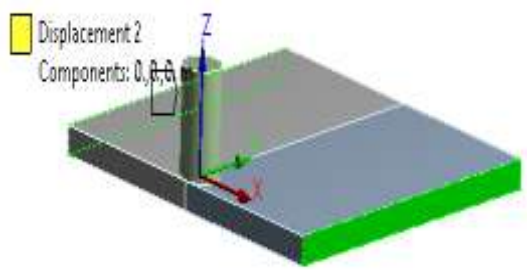

Figure 6: Mechanical Boundary Condition - Displacement 2

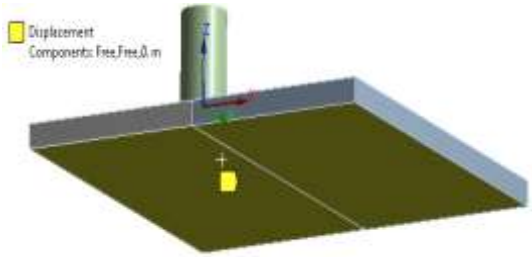

Figure 7: Mechanical Boundary Condition – Displacement

4.6 Loading

There are three main stages to the FSW process:

1. **Plunge** -- Slowly, the tool enters the work piece.
2. **Dwell** -- Friction between the spinning tool and the workpiece generates heat at the original tool site until the workpiece temperature reaches the required level for welding.
3. **Traverse (or Traveling)** -- Along the weld line, the spinning tool is in motion.

During the traverse phase, the temperature in the weld line region rises, but the peak temperature values do not surpass the melting point of the workpiece material. As the temperature decreases, the joint between the two plates becomes solid and continuous.

Each stage of the FSW process is viewed as a distinct load step for the sake of illustration. For the purpose of loading the tool, a hard surface constraint is already established.
The information for each load phase is displayed in Table 8 below.

Table 8: Details for each load step.

Load Step	Time Period (sec)	Loadings on Pilot Node	Boundary Condition
1	1	Displacement boundary condition	UZ = -1.06E-06 M
2	6.5	Rotational boundary condition	ROTZ = 50 RPM
3	29	Displacement and rotational boundary conditions together on the pilot node	ROTZ = 50 RPM UY = 60.96E-03 m

In this investigation, the depth of penetration was raised to see how it would affect the temperature and stress on the work piece.

Because of the material's plastic deformation and the friction between the tool's shoulder and the workpiece, heat is generated during the

second and third load phases, as evidenced by the observed temperature rise in the model.

Tool material melts at a temperature of 1450 °C. As shown in the accompanying Graph 1, the maximum temperature range at the weld line area on the workpiece beneath the tool during the second and third load phases is greater than 70% of the melting temperature. This temperature range is much below the workpiece material's melting point:

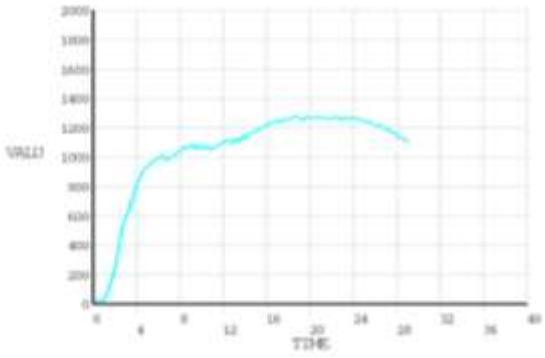

Graph 1: Maximum Temperature Variation with Time (on Workpiece Under the Tool).

The bonding temperature of 1000 °C is already set for the welding simulation at the plate contact. The contact condition at this interface after the last load step is shown in Figure 8 below.

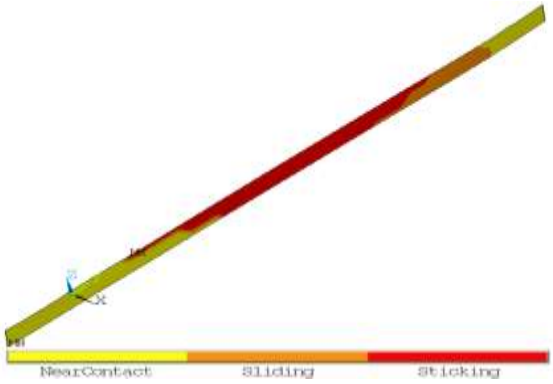

Figure 8: Following the last load, check the contact status at this interface.

The location where the plates are bonded or welded is seen in the sticking section of the interface. The welding zone would grow if the bonding temperature were set at 900 °C.

4.7 Heat Generation:

Heat is produced by friction and plastic deformation. Heat production from plastic and friction is calculated. In the second load step, friction starts to produce heat. The frictional heat generation on the workpiece is computed using the FDDIS (SMISC item) output option of the CONTA174 element. This choice provides the frictional energy dissipation per unit area for an element. By dividing this amount by the necessary element area, one may calculate the rate of friction heat generation for a certain element. Calculating the overall frictional heat production rate over a certain period of time requires adding together the numbers from each CONTA174 component of the workpiece. Calculating the whole frictional heat-generation rate at each time-step is achievable (ETABLE). The rate of overall frictional heat generation on the workpiece is shown against time in Graph 2 as follows: The graph shows that the second load step is when frictional heat first appears (after 1 second).

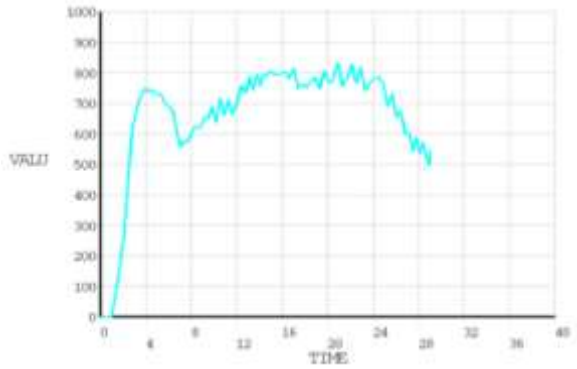

Graph 2: Total Frictional Heat Rate Variation with Time

5. RESEARCH RESULTS AND DISCUSSION

According to the table below, as penetration increases, stress rises by 146% for plunger penetration loading and by 5–10% for rotation loading.

Table 9: Stress in Case 1 and Case 2

Parameter	Case 1	Case 2	% Change
Depth of penetration (m)	7.95E-07	1.06E-06	-33%
Stress in LS1 (MPa)	19.8	48.7	-146%
Stress in LS2 (MPa)	300	328.9	-10%
Stress in LS3 (MPa)	550	578.9	-5%
Temp in LS2 (Deg C)	1001	1007	-6
Temp in LS3 (Deg C)	1090	1098	-8

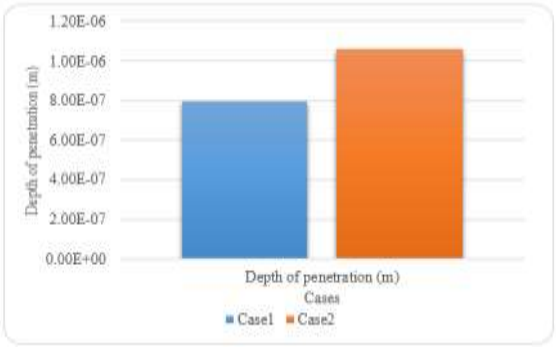

Graph 3: Depth of Penetration

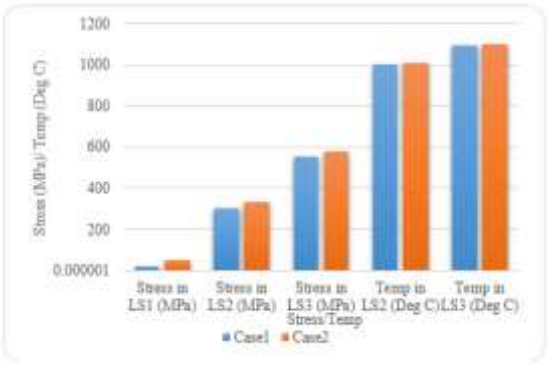

Graph 4: Stress vs Temp. graph

6. CONCLUSION

The greatest method for welding several aluminium alloys together over long distances with good quality is FSW. A lot of work is being put into utilising FSW to weld higher temperature materials such as steel and aluminium alloy alloys. Make the procedure far more adaptable by expanding it beyond its current usage of mostly basic butt and lap joint combinations.

The goal of the current experimental investigation is to assess the viability of FSW for two different materials: steel 304L and the AL alloy Al-5400. The experiment results are listed below.

1. Al-5400 and Steel 304L, two dissimilar materials, were effectively welded together utilising FSW at varying tool rotation rates, weld speeds, and probe offsets toward the Al-5400's softer side.
2. At 50 RPM, the impact of penetration depth is investigated, and it is discovered that the deeper the penetration, the more stress the work piece generates. Additionally, due to increased friction, the heat at the contact surface has increased, yet the temperature required to melt the work piece is sufficient to form the weld.

7. FUTURE SCOPE

- Impact of tool profile can be check
- Based on the best values, this analysis may also be used to anticipate the empirical equations that will allow the process to be automated.

REFERENCES

W. M. Thomas, Friction stir welding and related friction process characteristics, In Proc. 7th Int. Conf. on Joints in aluminium–INALCO. 98, (1998) 157-174.

R. S. Mishra, P. S. De, N. Kumar, Friction stir welding and processing: science and engineering. (2014), Springer, https://doi.org/10.1007/978-3-319-07043-8.

F. C. Liu, T. W. Nelson, Grain structure evolution, grain boundary sliding and material flow resistance in friction welding of Alloy 718, Materials Science and Engineering A. 710 (2018), 280-288, https://doi.org/10.1016/j.msea.2017.10.092.

W. M. Thomas, E. D. Nicholas, J. C. Needham, M. G. Murch, P. Smith-Temple, C. J. Dawes, Friction Welding, U.S. Patent No. 5,460.317, (Oct 24. 1995), https://patents.google.com/patent/US5460317A/en.

J. W. Arbegast, P. J. Hartley, Method of using friction stir welding to repair weld defects and to help avoid weld defects in intersecting welds, U.S. Patent No. 6,230,957, (May 15. 2001), https://patents.google.come/patent/US6230957B1/en.

S. M. Packer, R. J. Steel, J. A. Babb, C. Reed, B. E. Taylor, Crack repair using friction stir welding on materials including metal matrix composites, ferrous alloys, non-ferrous alloys, and superalloys, U.S. Patent No. 7,225.968, (5 Jun. 2007), https://patents.google.com/patent/US7225968B2/en.

K. Ross, B. Sutton, G. Grant, G. Cannell, G. Frederick, R. Couch, Development of friction stir processing for repair of nuclear dry cask storage system canisters, In Friction Stir Welding and Processing IX. (2017) 39- 46, Springer, https://doi.org/10.1007/978-3-319-52383-5_5.

C. Gunter, M. P. Miles, F. C. Liu, T. W. Nelson, Solid state crack repair by friction stir processing in 304L stainless steel, Journal of Materials Science and Technology. 34 (2018) 140- 147, https://doi.org/10.1016/j.jmst.2017.10.023.

G. Çam, Friction stir welded structural materials: beyond Al-alloys, International Materials Reviews. 56 (2011) 1-48, https://doi.org/10.1179/095066010X12777205875750.

M. Jafarzadegan, A. H. Feng, A. Abdollah-Zadeh, T. Saeid, J. Shen, H. Assadi, Microstructural characterization in dissimilar friction stir welding between 304 stainless steel and st37 steel, Materials Characterization. 74 (2012) 28-41, https://doi.org/10.1016/j.matchar.2012.09.004.

A. P. Reynolds, W. Tang, T. Gnaupel-Herold, H. Prask, Structure, properties, and residual stress of 304L

stainless steel friction stir welds, Scripta Materialia. 48 (2003) 1289-1294, https://doi.org/10.1016/S1359-6462(03)00024-1.

S. H. C. Park, Y. S. Sato, H. Kokawa, K. Okamoto, S. Hirano, M. Inagaki, Microstructural characterization of stir zone containing residual ferrite in friction stir welded 304 austenitic stainless steel, Science and Technology of Welding and Joining. 10 (2005) 550-556, https://doi.org/10.1179/174329305X46691.

Y. S. Sato, T.W. Nelson, C. J. Sterling, Recrystallization in type 304L stainless steel during friction stirring, Acta Materialia. 53 (2005) 637-645, https://doi.org/10.1016/j.actamat.2004.10.017.

T. Saeid, A. Abdollah-Zadeh, T. Shibayanagi, K. Ikeuchi, H. Assadi, On the formation of grain structure during friction stir welding of duplex stainless steel, Materials Science and Engineering: A, 527 (2010) 6484-6488, https://doi.org/10.1016/j.msea.2010.07.011.

T. Saeid, A. Abdollah-Zadeh, H. Assadi, F. M. Ghaini, Effect of friction stir welding speed on the microstructure and mechanical properties of a duplex stainless steel, Materials Science and Engineering: A. 496 (2008) 262-268, https://doi.org/10.1016/j.msea.2008.05.025.

H. Fujii, L. Cui, N. Tsuji, M. Maeda, K. Nakata, K. Nogi, Friction stir welding of carbon steels, Materials Science and Engineering: A. 429 (2006) 50-57, https://doi.org/10.1016/j.msea.2006.04.118.

T. J. Lienert, W. L. Stellwag Jr, B. B. Grimmett, R. W. Warke, Friction stir welding studies on mild steel, Welding Journal-New York. 82 (2003) 1-9S.

A. Ozekcin, H. W. Jin, J. Y. Koo, N. V. Bangaru, R. Ayer, G. Vaughn, S. Steel, S. Packer, A microstructural study of friction stir welded joints of carbon steels, International Journal of Offshore and Polar Engineering. 14 (2004).

A. K. Lakshminarayanan, V. Balasubramanian, M. Salahuddin, Microstructure, tensile and impact toughness properties of friction stir welded mild steel, Journal of Iron and Steel Research International. 17 (2010) 68-74, https://doi.org/10.1016/S1006-706X(10)60186-0.

Y. D. Chung, H. Fujii, R. Ueji, N. Tsuji, Friction stir welding of high carbon steel with excellent toughness and ductility, Scripta Materialia. 63 (2010) 223-226, https://doi.org/10.1016/j.scriptamat.2010.03.060.

C. Meran, V. Kovan, A. Alptekin, Friction stir welding of AISI 304 austenitic stainless steel, Material wissenschaft und Werkstofftechnik: Entwicklung, Fertigung, Prüfung, Eigenschaften und Anwendungen Technischer Werkstoffe. 38 (2007) 829-835, https://doi.org/10.1002/mawe.200700214

G. Çam, G. İpekoğlu, T. Küçükömeroğlu, S. M. Aktarer, S. M, Applicability of friction stir welding to steels, Journal of Achievements in Materials and Manufacturing Engineering. 80 (2017), https://doi.org/10.5604/01.3001.0010.2027.

D G Mohan, S Gopi. Induction assisted friction stir welding: A review. Australian Journal of Mechanical Engineering, 2020, 18(1): 119–123.

L Cui, C Zhang, Y Liu. Recent progress in friction stir welding tools used for steels. J. Iron Steel Res. Int., 2018, 25: 477–486.

D G Mohan, S Gopi, V Rajasekar. Effect of induction heated friction stir welding on corrosive behaviour, mechanical properties and microstructure of AISI 410 stainless steel. Indian Journal of Engineering and Materials Sciences, 2018, 25(3): 203–208.

H Fujii, L Cui, K Nakata. Mechanical properties of friction stir welded carbon steel joints — Friction stir welding with and without transformation. Weld World, 2008, 52: 75–81.

E Reza, M Rabby, K Ross, et al. Solid-state joining of thick-section dissimilar materials using a new friction stir dovetailing (FSD) process. Minerals, Metals and Materials Series, 2017, 9783319523828: 67–77.

A I Álvarez, M García, G Pena, et al. Evaluation of an induction-assisted friction stir welding technique for super duplex stainless steels. Surface and Interface Analysis, 2014, 46(10–11): 892–896.

A Sasikumar, S Gopi, D G Mohan. Effect of welding speed on mechanical properties and corrosion resistance rates of filler induced friction stir welded AA6082 and AA5052 joints. Mater. Res. Express, 2021, 8(6): 066531.

A Sasikumar, S Gopi, D G Mohan. Effect of magnesium and chromium fillers on the microstructure and tensile strength of friction stir welded dissimilar aluminium alloys. Materials Research Express, 2019, 6(8).

N A Muhammad, C Wu, G K Padhy. Review: Progress and trends in ultrasonic vibration assisted friction stir welding. Journal of Harbin Institute of Technology (New Series), 2018, 25(3): 16–42.

P Xue, X Zhang, L Wu, et al. Research progress on friction stir welding and processing. Acta Metallurgica Sinica, 2016, 52(10): 1222–1238.

Y Zhang, Y S Sato, H Kokawa, et al. Stir zone microstructure of commercial purity titanium friction stir welded using PCBN tool. Mater. Sci. Eng.-Lausanne- A, 2008, 488(1–2): 25–30.

B Mortazavi, G Cuniberti. Mechanical properties of polycrystalline boron-nitride nanosheets. RSC Advances, 2014, 4(37): 19137–19143.

M A Siddiqui, S Jafri, P Bharti, et al. Friction stir welding as a joining process through modified conventional milling machine: A review International Journal of Innovative Research & Development, 2014, 3(7): 149–153.

G K Padhy, C S Wu, S Gao. Auxiliary energy assisted friction stir welding – Status review. Science and Technology of Welding and Joining, 2015, 20(8): 631–649.

M Imam, R Ueji, H Fujii. Effect of online rapid cooling on microstructure and mechanical properties of friction stir welded medium carbon steel. Journal of Materials Processing Technology, 2016, 230: 62–71.

Y M Hwang, C H Lin. Friction stir welding of dissimilar metal sheets. Steel Research International, 2010, 81(9): 1076–1079.

A Mishra. A review on the effect of cryogenic treatment on the mechanical properties of friction stir welded joints. Journal of Advanced Research in Mechanical Engineering and Technology, 2019, 5(3–4): 24–27.

K K Jangra, N Sharma, R Khanna, et al. An experimental investigation and optimization of friction stir welding process for AA6082 T6 (cryogenic treated and untreated) using an integrated approach of Taguchi, grey relational analysis and entropy method. Procee-dings of the Institution of

Mechanical Engineers, Part L: Journal of Materials: Design and Applications, 2016, 230(2): 454–469.

P Baillie, S W Campbell, A M Galloway, et al. Friction stir welding of 6mm thick carbon steel underwater and in air. Science and Technology of Welding and Joining, 2015, 20(7): 585–593.

A Banik, J D Barma, R Singh, et al. A study on the effect of varying revolution pitch for different tool design: Friction stir welding of AA 6061-T6.

In: K Shanker, R Shankar, R Sindhwani, eds. Advances in industrial and production engineering. Lecture Notes in Mechanical Engineering, Springer, Singapore, 2019.

L N Brewer, M S Bennett, B W Baker, et al. Characterization of residual stress as a function of friction stir welding parameters in oxide dispersion strengthened (ODS) steel MA956. Materials Science and Engineering: A, 2015, 647: 313–321.

H Dawson, M Serrano, S Cater, et al. Residual stress distribution in friction stir welded ODS steel measured by neutron diffraction. Journal of Materials Processing Technology, 2017, 246: 305–312.

H Dawson, M Serrano, R Hernandez, et al. Mechanical properties and fracture behaviour of ODS steel friction stir welds at variable temperatures. Materials Science and Engineering: A, 2017, 693: 84–92

A K Lakshminarayanan, V Balasubramanian. Characteristics of laser beam and friction stir welded AISI 409M ferritic stainless steel joints. Journal of Materials Engineering and Performance, 2012, 21(4): 530–539.

T Wang, M Komarasamy, S Shukla, et al. Simultaneous enhancement of strength and ductility in an AlCoCrFeNi2.1 eutectic high-entropy alloy via friction stir processing. Journal of Alloys and Compounds, 2018, http://:766:312–317 .

A Tribe, T W Nelson. Study on the fracture toughness of friction stir welded API X80. Engineering Fracture Mechanics, 2015, 150: 58–69.

M Esmailzadeh, M Shamanian, A Kermanpur, et al. Microstructure and mechanical properties of friction stir welded lean duplex stainless steel. Materials Science and Engineering: A, 2013, 561: 486–491.

J Jeon, S Mironov, Y S Sato, et al. Anisotropy of structural response of single crystal austenitic stainless steel to friction stir welding. Acta Materialia, 2013, 61(9): 3465–3472.

Y C Chen, H Fujii, T Tsumura, et al. Banded structure and its distribution in friction stir processing of 316L austenitic stainless steel. Journal of Nuclear Materials, 2012, 420(1–3).

A K Lakshminarayanan, V Balasubramanian. Assessment of sensitization resistance of AISI 409M grade ferritic stainless steel joints using modified Strauss test. Materials & Design, 2012, 39: 175–185.

D M Sekban, S M Aktarer, P Xue, et al. Impact toughness of friction stir processed low carbon steel used in shipbuilding. Materials Science and Engineering: A, 2016, 672: 40–48.

Y Sun, H Fujii, H Imai, et al. Suppression of hydrogen-induced damage in friction stir welded low carbon steel joints. Corrosion Science, 2015, 94: 88–98.